Journal of CO2 Utilization 102 (2025) 103270

Contents lists available at ScienceDirect

Journal of CO2 Utilization

journal homepage: www.elsevier.com/locate/jcou

Tuning catalyst performance in methane dry reforming via microwave irradiation of Nickel-Silicon carbide systems

Christel Olivier Lenge Mbuya [a], Kunal Pawar [a], Mitra Jafari [a], Parisa Shafiee [a], Chike George Okoye Chine [b], Pilar Tarifa [c], Bogdan Dorneanu [a], Harvey Arellano-Garcia [a,*]

[a] Fachgebiet Prozess- und Anlagentechnik, Brandenburg University of Technology Cottbus-Senftenberg, Cottbus, Germany
[b] Global R&D, Avery Dennison Corporation, 171 Draketown Road, Mill Hall, PA 17751, United States
[c] Instituto de Nanociencia y Materiales de Aragón (INMA), CSIC-U de Zaragoza, C/Mariano Esquillor s/n, Zaragoza 50018, Spain

ARTICLE INFO

Keywords:
Carbon dioxide
Dry reforming
Methane
Microwave irradiation
Ni Silicon carbide catalysts

ABSTRACT

The dry reforming of methane (DRM) is a promising route for converting greenhouse gases such as methane (CH_4) and carbon dioxide (CO_2) into valuable syngas, hydrogen (H_2) and carbon monoxide (CO). However, traditional nickel (Ni)-based catalysts suffer from rapid deactivation due to carbon deposition and sintering, especially when supported on low thermal conductivity materials. In this work, a novel post-synthesis microwave irradiation (MIR) treatment is introduced to systematically optimize the performance of Ni – β – SiC and Ni – Ti – Cβ – SiC catalysts for DRM. Unlike previous studies that have used MIR during reaction or with different supports, this approach tunes the metal – support interactions and textural properties of Ni – β – SiC and Ni – Ti – Cβ – SiC catalysts by varying the MIR exposure time after catalyst synthesis. MIR post-treatment (10–25 s) increased the CH_4 conversion to 65 % and the CO_2 conversions to 62 % for Ni–β–SiC catalysts and improved the H_2/CO ratio to 0.80, with stable performance over 20 h. For Ni–Ti–Cβ–SiC, MIR (10–20 s) maintained CH_4 conversion up to 60 % and CO_2 conversion to 58 % over 20 h, while the untreated catalyst, though initially higher, deactivated rapidly. Excessive MIR (30 s) reduced performance for both catalyst types, underscoring the need for optimal exposure time. These findings demonstrate post-synthesis MIR provides a tuneable approach for enhancing both the activity and durability of Ni/SiC – based DRM catalysts through controlled modification of metal – support interactions. This work offers new insights for the design of robust catalysts aimed at greenhouse gas utilization and sustainable syngas production, with activity and stability enhancements linked to controlled changes in metal – support interactions.

1. Introduction

Nowadays, governments are introducing and implementing policies that aim to reduce carbon emissions in the atmosphere and shift towards cleaner and sustainable energies [1]. Both methane (CH_4) and carbon dioxide (CO_2) are greenhouse gases (GHGs) that contribute to increasing the temperature in the atmosphere [2]. Their accumulation mostly comes from industrial activities, therefore, they can be reduced and valorised from an environmental and economic point of view, by combining CH_4 and CO_2 in the presence of a catalyst to produce a mixture of carbon monoxide (CO) and hydrogen (H_2) called syngas [3]. This reaction is known as the CH_4 dry reforming (DRM) as shown in Eq. (1). It is an endothermic reaction that absorbs heat from the surroundings [4].

$$CH_4 + CO_2 \leftrightarrow 2CO + 2H_2 \quad (1)$$

The syngas (CO/H_2) can be used to generate electricity using a gas turbine or can be used as feedstock for the Fischer-Tropsch synthesis (FTS) to produce liquid fuels [5], methanol (CH_3OH) [6], or dimethyl ether (DME) [7]. Etc.

Nickel (Ni) is the active phase for the DRM and can be supported on alumina (Al_2O_3), zeolites, and silica (SiO_2) because of their high surface areas which allow high dispersion of the Ni [8] [9]. The major problems of the DRM's catalysts are Ni sintering and coking from the surface, which is due to the low thermal conductivity of the Al_2O_3 and SiO_2, and the high temperatures required for DRM, which are between 700 and 800 °C [4,10,11]. The formation of carbon filament on traditional Ni catalysts also leads to clogging of the reactor [12].

A variety of strategies have been implemented to reduce coke

* Corresponding author.
E-mail address: arellano@b-tu.de (H. Arellano-Garcia).

https://doi.org/10.1016/j.jcou.2025.103270
Received 16 July 2025; Received in revised form 22 September 2025; Accepted 30 October 2025
Available online 5 November 2025

formation during DRM. These include the design of bimetallic catalysts, where, for example, the redox properties of Fe in Ni-Fe systems facilitate more effective interaction with surface carbon and thus reduce coking [13]. Likewise, Ni-Rh bimetallic catalysts form Ni-Rh clusters which suppress carbon formation [13]. Another effective approach involves supports with a high density of oxygen vacancies, such as basic metal oxides like La_2O_3, which enhance CO_2 adsorption and directly interact with deposited carbon species to mitigate coking [13]. These diverse methods complement MIR optimization and offer avenues for robust, coke-resistant catalyst design.

Beta silicon carbide (β-SiC) could be used as a catalyst support for DRM because of its hardness and high thermal conductivity that could help stabilize the Ni active phase at high temperatures [14,15]. Due to its small surface area (10–40 m^2/g), and the weak interaction between the metal and the support [14], β-SiC catalyst is not as efficient as high surface area supports such as Al_2O_3 and SiO_2. Catalyst manufacturing companies and academia focus on the modification of β-SiC supports to improve its properties for catalysis.

The efficiency of β-SiC was demonstrated in the DRM by Silva et al. [12], in a study of the effect of supports, and they showed that Ni-β-SiC-based catalysts were more active and stable, with less carbon deposition than Ni-Al_2O_3 and Ni-SiO_2, because the high thermal conductivity of β-SiC provided higher stability of the Ni active phase. Zhang et al. [16], investigated the catalytic performance of a Ni-La_2O_3/SiC foam catalyst at 850°C for the DRM process. This catalyst showed a CH_4/CO_2 conversion of 71 %/85 % at the beginning of the reaction, which decreased to 60 %/72 % after 50 h on stream, and remained unchanged for the next 50 h, while a Ni-La_2O_3/Al_2O_3 catalyst CH_4/CO_2 conversions were 49 %/71 % and decreased rapidly to 24 %/40 % after 25 h on stream due to higher carbon deposition and Ni sintering.

From these observations, it would be worthy investigating the possibility to improve the performance of Ni-β-SiC catalysts, since both Ni and β-SiC are known as good microwave absorber compounds [17,18]. Hence, the catalyst properties could be tuned by exposing them to microwave irradiation (MIR) [15]. MIR has been widely used in the past to improve the performance of heterogeneous catalysts [19,20]. Among the benefits of MIR in gas phase reaction catalysis, improved conversions, selectivity, and stability of the reaction can be mentioned. Fidalgo et al. [21], have reported higher CH_4 and CO_2 conversion for DRM using MIR heating compared to conventional heating. In their study, activated carbon served both as catalyst and the MIR receptor or absorber.

This paper presents a novel strategy for enhancing the performance of the Ni-β-SiC and its modified counterpart, Ni-Ti-Cβ-SiC, catalysts for DRM. Unlike previous studies, MIR is employed as a post-synthesis treatment, systematically investigating its impact on catalyst properties and performance. By optimizing the MIR exposure time after calcination, the aim is to induce beneficial changes in the bulk structure of the catalysts, potentially unlocking new pathways for improving catalytic activity and stability. To our knowledge, this is among the first studies to apply MIR post-treatment to Ni-β-SiC-based catalysts for DRM, offering fresh insights into the role of MIR in tuning catalyst-support interactions and enhancing DRM efficiency.

The remainder of the paper is organized as follows: Section 2 describes the materials, catalyst preparation procedures, and the MIR post-synthesis treatment protocol. Section 3 details the characterization techniques used to analyse the structural, textural, and chemical properties of the catalysts. Section 4 discusses the experimental results, focusing on the effects of MIR treatment on catalyst structure, reducibility, and DRM performance, as well as the optimization of MIR exposure time. Finally, Section 6 summarizes the main findings and outlines future research directions.

2. Experimental

2.1. Chemicals and materials

All materials were used as received, without further purification. Beta silicon carbide (β-SiC) and titania carbon enriched with beta silicon carbide (Ti-Cβ-SiC) extrudates (2 mm) were obtained from SICAT (Germany). Nickel nitrate hexahydrate ($Ni(NO_3)_2{\cdot}6H_2O$, 98 %, Thermo Fischer Scientific) was used as the Ni precursor. Deionised water was employed for all catalyst preparation procedures. A domestic microwave oven instrument (TEC) operating at 700 W and frequency of 2.45 GHz was utilised to perform the post-synthesis MIR treatment of the Ni silicon carbide catalysts. This basic type of microwave oven does not have options to measure the temperature profiles of the samples during irradiation. Treatments were carried out at room atmosphere with the catalyst powders spread uniformly in petri dishes to ensure even exposure.

2.2. Catalysts preparation of nickel supported silicon carbide catalysts

The β-SiC and Ti-Cβ-SiC supports were crushed and sieved using test sieves to obtain a uniform particle size of 100 μm. This size reduction was performed to enhance MIR penetration, as finer particles allow for more effective interaction with microwave radiation compared to extrudates [22], thereby ensuring uniform treatment across the catalyst samples.

For the preparation of the Ni-β-SiC catalysts, 26.77 g of Ni $(NO_3)_2{\cdot}6H_2O$ was dissolved in 45 mL of deionised water. Similarly, for the Ni-Ti-Cβ-SiC catalysts, 26.77 g of $Ni(NO_3)_2{\cdot}6H_2O$ was dissolved in 30.6 mL deionised water. Each nickel nitrate solution was impregnated onto 36 g of the respective support using the incipient wetness impregnation method, targeting a nominal Ni loading of 15 wt% for both catalyst systems.

After impregnation, the catalysts were dried in a water bath (Bandelin Sonorex Super RK 156BH) at 80 °C for 5 h to gradually remove the solvent, followed by further drying in an oven (Heraeus) at 120 °C for 5 h to ensure complete moisture removal. The dried samples were subsequently calcined in static air at 550 °C for 4 h to decompose the nitrate precursor and form the oxide phase.

For the MIR post-synthesis treatment, 5 g of each calcined catalyst was uniformly spread in a petri dish and subjected to MIR at 700 W for varying durations (10, 15, 20, 25, and 30 s), as illustrated in Fig. 1. The resulting samples were designated according to their support type and MIR exposure time, as summarised in Table 1. To estimate the rise of temperature upon MIR treatment, a thermocouple and temperature controller (ALMEMO 3290] were used to measure the sample surface temperature immediately after irradiation. These measurements confirmed that temperature increases with exposure time. For identical exposure times, Ni-Ti-Cβ-SiC samples exhibit higher post-MIR temperatures compared to Ni-β-SiC, attributed to enhanced microwave absorption by both the carbon (activated) and the β-SiC phases (see Supplementary Information Table S2).

2.3. Characterizations

A comprehensive suite of characterization techniques was employed to identify the structural, textural and chemical properties of the prepared catalysts.

2.3.1. X-ray diffraction (XRD)

X-ray diffraction (XRD) analysis was performed to identify the crystalline phases present in the catalyst supports and to characterize the Ni active species. Diffraction patterns were collected using a Brukers D2 powder diffractometer with Cu-Kα radiation ($\lambda = 1.5406$ Å), scanning over a 2θ range of 5°– 80° at a step rate of 0.15°/min. The average crystallite size of Ni was estimated from the XRD data using the Scherrer

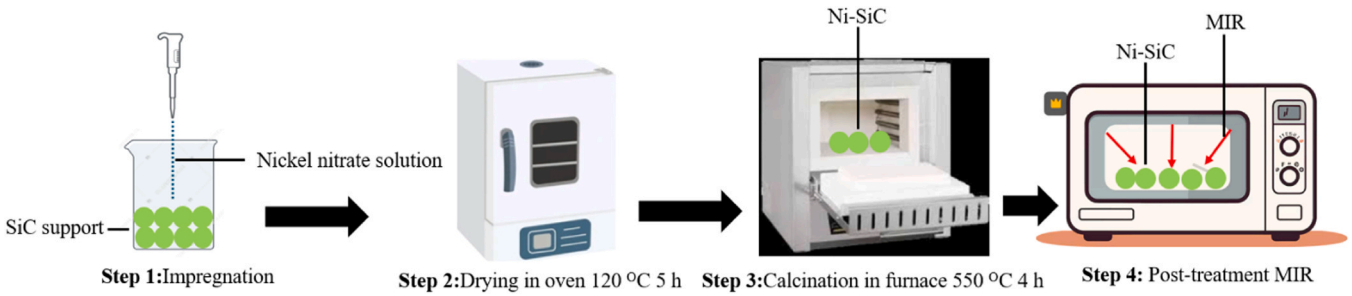

Fig. 1. Microwave post-treatment of Ni silicon carbide catalysts.

Table 1
Ni silicon carbide catalysts and optimization procedure.

MIR exposure time (s)	Catalysts
0	Ni-β-SiC (0 s), untreated
10	Ni-β-SiC (10 s)
15	Ni-β-SiC (15 s)
20	Ni-β-SiC (20 s)
25	Ni-β-SiC (25 s)
30	Ni-β-SiC (30 s)
0	Ni-Ti-Cβ-SiC (0 s)
10	Ni-Ti-Cβ-SiC (10 s)
15	Ni-Ti-Cβ-SiC (15 s)
20	Ni-Ti-Cβ-SiC (20 s)
25	Ni-Ti-Cβ-SiC (25 s)
30	Ni-Ti-Cβ-SiC (30 s)

equation.

2.3.2. Temperature programmed reduction (TPR)

The TPR experiments were conducting on a ChemBET Pulsar instrument to evaluate the reducibility of the catalysts and the interaction between Ni active phase and the SiC-based supports. Approximately 50 mg of catalyst was loaded into a U-shaped quartz reactor. The sample was subjected to a flow of 10 % H_2 in N_2 (total flow rate: 50 mL/min) while being heated from 25°C to 900°C at a rate of 10 °C/min. Hydrogen conduction was monitored using a thermal conductivity detector (TCD).

2.3.3. Nitrogen physisorption

Textural properties of the catalysts, including specific surface area, pore volume, and average pore diameter, were determined by nitrogen physisorption using a Micromeritics ASAP 2460 instrument. Prior to analysis, samples were degassed at 160°C for 12 h under vacuum. Surface areas were calculated using the Brunauer-Emmett-Teller (BET) method, while pore size distributions and pore volumes were derived from the adsorption branch of the isotherm using the Barrett-Joyner-Halanda (BJH) method.

2.4. Catalytic testing

Catalytic performance in the DRM reaction was evaluated in a fixed-bed reactor system, as illustrated in Fig. 2. The length of the reactor tube was 23 cm, and 0.9 cm internal diameter (ID). Single measurements were performed for each catalyst due to the high number of samples and availability of the reactor set up.

For each test, 0.2 g of catalysts was loaded into the reactor. Prior to reaction, catalysts were reduced in situ under a flow of H_2/N_2 (10 %/90 %) at a total flow rate of 142 mL/min. Ni-β-SiC catalysts were reduced at 700 °C, while Ni-Ti-Cβ-SiC catalysts were reduced at 400 °C, each for 2 h. The reduction temperatures were assessed based on the H_2-TPR measurements shown in the Fig. 4(a) and (b).

The DRM reaction was conducted at 700 °C for 20 h, using a feed gas mixture of CH_4, CO_2, and N_2 in a 1:1:1 molar ratio. Product gases (CH_4, CO_2, CO and H_2) were analysed using an SSM 6000 gas analyser. The

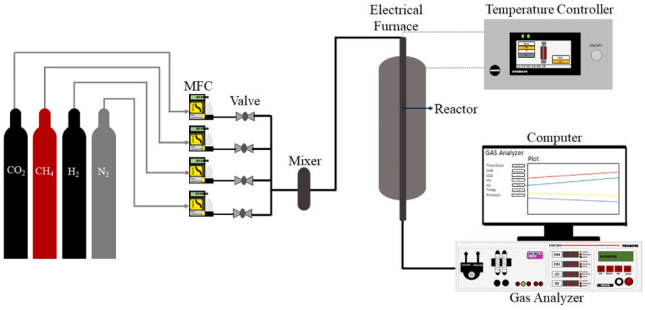

Fig. 2. DRM laboratory set up.

CH_4, CO_2 conversions, as well as product selectivities, were calculated according to the following equations:

$$X_i = \left(\frac{Molar\ flow\ rate_{i,in} - Molar\ flow\ rate_{i,out}}{Molar\ flow\ rate_{i,in}} \right) \times 100\% \quad (2)$$

$$\text{Yield of} H_2 = \left(\frac{Moles\ of H_2 produced}{Molar\ flow\ rate_{CH4,in}} \right) \times 100\% \quad (3)$$

$$H_2 / \text{CO Ratio} = \frac{Moles\ of H_2 produced}{Moles\ of\ CO\ produced} \quad (4)$$

Carbon quantification was performed by collecting and weighing the carbon residue isolated after 20 h of DRM reaction, using the mass difference method for post-reaction samples. The protocol and data can be found in Table S1 of the Supplementary Information. Comprehensive morphological and structural characterization of carbon species, such as differentiation of nanotubes, amorphous, or graphitized carbon, using SEM and Raman spectroscopy will be addressed in subsequent studies.

These procedures enabled a systematic evaluation of the effect of MIR post-synthesis treatment on catalyst structure and DRM performance.

3. Results and discussions

3.1. Characterizations

BET surface area measurements revealed that the Ti-Cβ-SiC support exhibited a significantly higher surface area (79.66 m^2/g) than β-SiC (29.45 m^2/g), although its pore volume was lower, as detailed in Table 2. The higher surface area of Ti-Cβ-SiC facilitated improved dispersion of Ni particles, as confirmed by elemental mapping (see Supporting Information S1). Titania (Ti) in the Ti-Cβ-SiC support also enhanced the interaction between Ni and support. The measured surface area for β-SiC aligns with values reported for commercial β-SiC extrudates [23].

After Ni impregnation, the surface area of most samples stabilized around 30 m^2/g, except for the Ni-β-SiC (10 s) catalyst, which showed a

Table 2
Textural properties of Ni silicon carbide catalysts.

Catalysts	Surface area (m^2/g)	Pore volume (cm^3/g)	Pore diameter (nm)	Crystallites size (nm)
β-SiC	29.02	0.109	15.00	-
Ni-β-SiC (0 s)	30.96	0.139	17.93	18.66
Ni-β-SiC (10 s)	44.01	0.180	16.34	17.42
Ni-β-SiC (15 s)	31.13	0.140	17.84	17.08
Ni-β-SiC (20 s)	25.61	0.109	17.17	17.27
Ni-β-SiC (25 s)	30.43	0.108	14.21	16.25
Ni-β-SiC (30 s)	31.56	0.140	17.70	17.55
Ti-Cβ-SiC	79.66	0.080	4.20	-
Ni-Ti-Cβ-SiC (0 s)	18.00	0.060	13.45	20.73
Ni-Ti-Cβ-SiC (10 s)	19.15	0.060	13.45	20.35
Ni-Ti-Cβ-SiC (15 s)	18.79	0.060	13.69	20.00
Ni-Ti-Cβ-SiC (20 s)	19.66	0.070	13.87	20.94
Ni-Ti-Cβ-SiC (25 s)	17.77	0.060	13.90	20.74
Ni-Ti-Cβ-SiC (30 s)	19.43	0.070	13.44	20.39

maximum surface area of 44 m^2/g and increased pore volume. This enhancement is attributed to the formation of additional pores, likely due to NiO particles residing outside the support pores, a consequence of the low surface area and inertness of β-SiC. For Ti-Cβ-SiC support, Ni impregnation led to a substantial decrease in both surface area (down to 18 m^2/g) and pore volume, indicating Ni incorporation within the support pores. Furthermore, MIR exposure did not significantly alter these textural properties.

XRD patterns (Fig. 3) confirmed the presence of characteristic peaks for both supports and Ni phases: the diffraction peaks at $2\theta = 35.7°$, 41.5°, 60.2° and 72° are associated with β-SiC and Ti-Cβ-SiC supports [24], while the peaks at $2\theta = 37.2°$, 43.5°, 60.2° are associated to the Ni phases.

Ni crystallites size, calculated using the Scherrer equation based on the most intense Ni diffraction peak, located at 43.5°, were approximately 17 nm for Ni-β-SiC and increased to 20 nm for Ni-Ti-Cβ-SiC. Notably, MIR exposure did not significantly affect Ni crystallite size, suggesting that Ni is largely transparent (does not absorb) to MIR and the catalytic changes are mainly due to the MIR-absorbing β-SiC support.

The distribution of elements or particles (Ni, Si, Ti, C, O) composing the Ni-Ti-Cβ-SiC catalysts were investigated through elemental mapping analysis obtained from SEM measurements, as shown in Fig. 4. For the untreated Ni-Ti-Cβ-SiC (0 s) catalyst, Ni and Si particles in oxide forms appeared well dispersed, while small areas of carbon were also present. The Ti was detected and likely positioned beneath other elements such as Ni and Si. Upon 10 s MIR exposure, extensive carbon-rich areas were observed on the catalyst surface, while at 15 s, Ni and Si predominated on the surface. Further MIR exposure for 20 and 25 s resulted in even larger carbon regions, and at 30 s, Ni and Si returned as the major surface species. These findings collectively suggest that varying MIR exposure time drives surface migration of species and thus modifies the form and distribution of Ni phases.

Similarly, the elemental mapping of Ni-β-SiC catalysts (Fig. 5) demonstrates that 10 s MIR exposure produces the most pronounced change, with particles presenting in a more oxidized state than in other Ni-β-SiC samples.

These observations provide direct evidence that MIR alters the

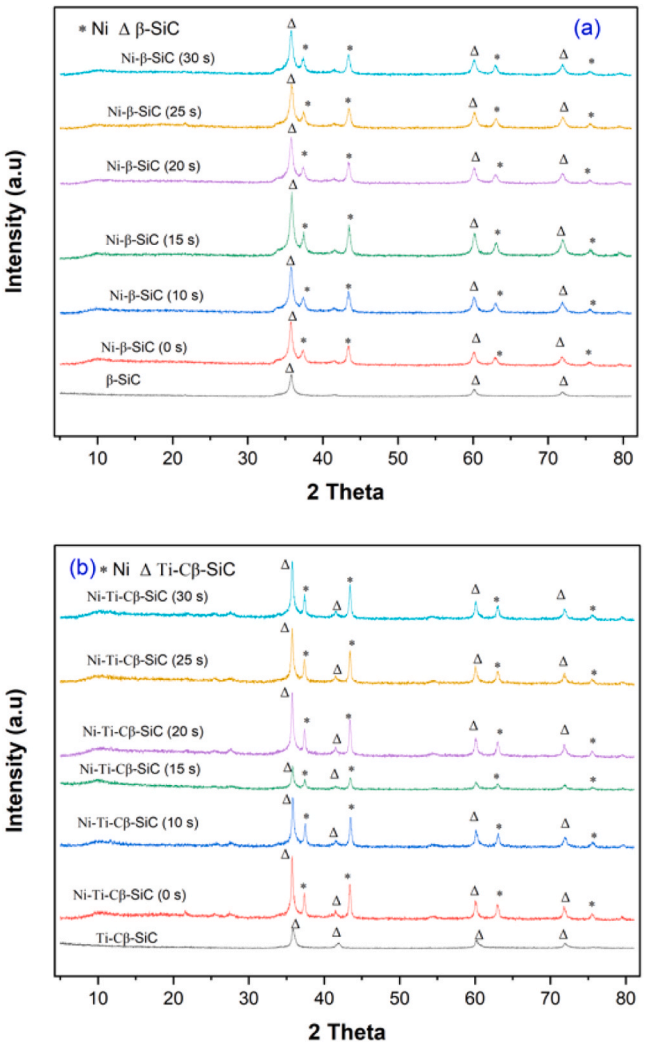

Fig. 3. XRD of: (a) Ni-β-SiC catalysts; (b) Ni-Ti-Cβ-SiC catalysts.

distribution and surface composition of catalyst species, which can be attributed to phase migration or transformation effects mediated by the irradiation process.

H_2-TPR profile of Ni-β-SiC (Fig. 6(a)) showed two main reduction peaks: α-type (between 200°C and 500°C), reflecting weaker NiO and β-SiC interaction, and β-type (between 600°C and 800°C), corresponding to stronger interactions [24]. MIR shifted the α-type reduction to lower temperatures, indicating weakened interactions, while β-type reduction shifted to higher temperatures, most prominently the Ni-β-SiC (10 s) catalyst, suggesting strengthened interactions at elevated temperatures relevant to DRM. In this study, the concept of strong or weak metal-support interactions is attributed to electron transfer processes from the supports (β-SiC and Ti-Cβ-SiC) to the Ni active phase during high-temperature reduction. MIR exposure modifies the distribution and electronic interaction of Ni on the supports, with more effective electron transfer stabilising Ni on β-SiC, while on Ti-Cβ-SiC, MIR reduces electron transfer. These findings are corroborated by TPR peak shifts Fig. 6 and elemental mapping results in Figs. 4 and 5.

For Ni-Ti-Cβ-SiC catalysts, H_2-TPR in Fig. 6(b) revealed reduction peaks between 200°C and 450°C, ascribed to the reduction of Ni^{2+} to Ni^0, with no higher-temperature features [25]. MIR exposure generally shifted reduction to lower reduction temperature. The microwaved Ni-Ti-Cβ-SiC catalysts that clearly shifted to a lower reduction temperature, indicating weakened Ni-support interactions, except for the Ni-Ti-Cβ-SiC (25 s) catalyst, which exhibited a shift to higher

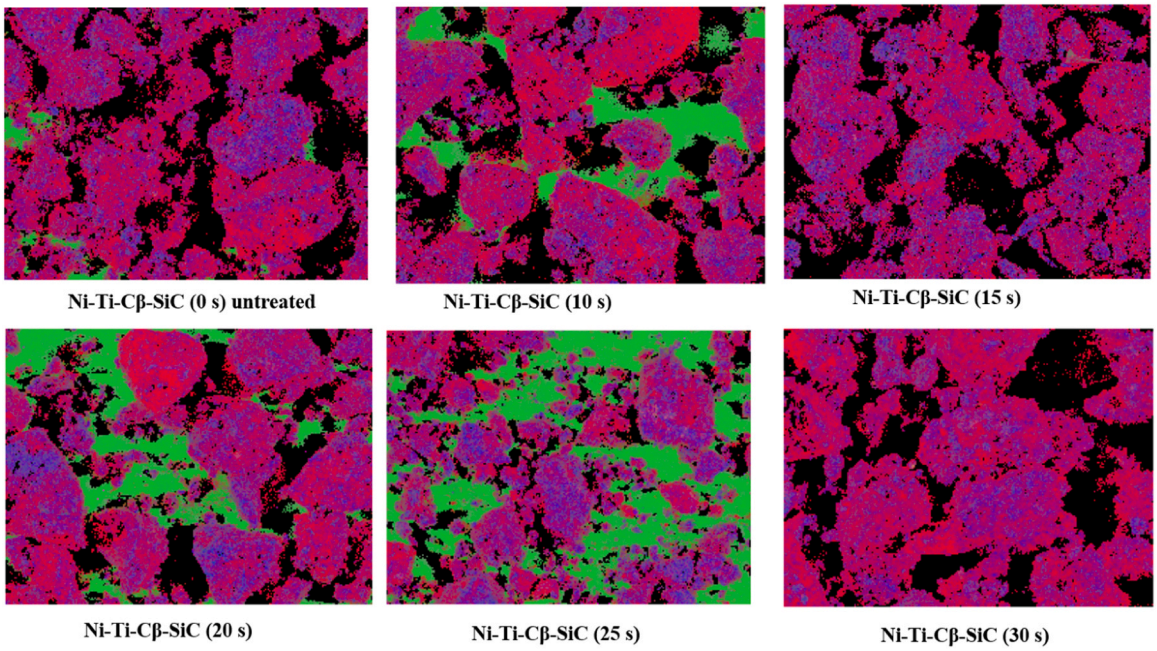

Fig. 4. Elemental mapping of Ni-Ti-Cβ-SiC catalysts (Ni ,Si ,C ,Ti , O_2).

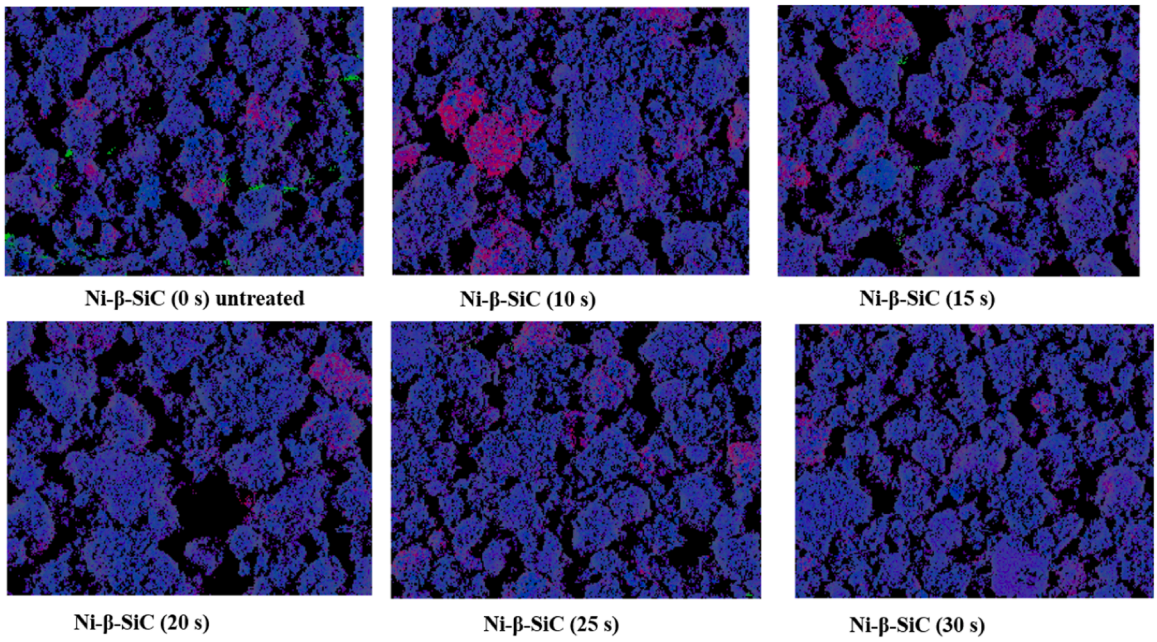

Fig. 5. Elemental mapping of Ni-β-SiC catalysts (Ni ,Si ,C , O_2).

temperature. In this case, the MIR reduced electron transferred from the Ti-Cβ-SiC support to the Ni particles. Overall, MIR treatment modulated the reducibility and metal-support interactions, with effects dependent on support composition and MIR exposure time.

3.2. Catalytic performance

3.2.1. Untreated catalysts: activity vs. stability trade-off

Prior to investigating the effect of MIR post-treatment, the intrinsic catalytic activity of the different Ti-Cβ-SiC- and β-SiC-supported Ni catalysts were evaluated under DRM conditions. As shown in Fig. 7(a) and (b), the Ni-Ti-Cβ-SiC catalyst achieved higher initial CH_4 conversion of 65 % and CO_2 conversion of 60 % compared to Ni-β-SiC catalyst with CH_4 conversion of (55 %) and CO_2 conversion of 50 %. However, Ni-β-SiC displayed greater stability throughout the reaction, while Ni-Ti-Cβ-SiC experienced a more pronounced deactivation after approximately 15 h on stream.

The superior activity of Ni-Ti-Cβ-SiC can be attributed to its higher

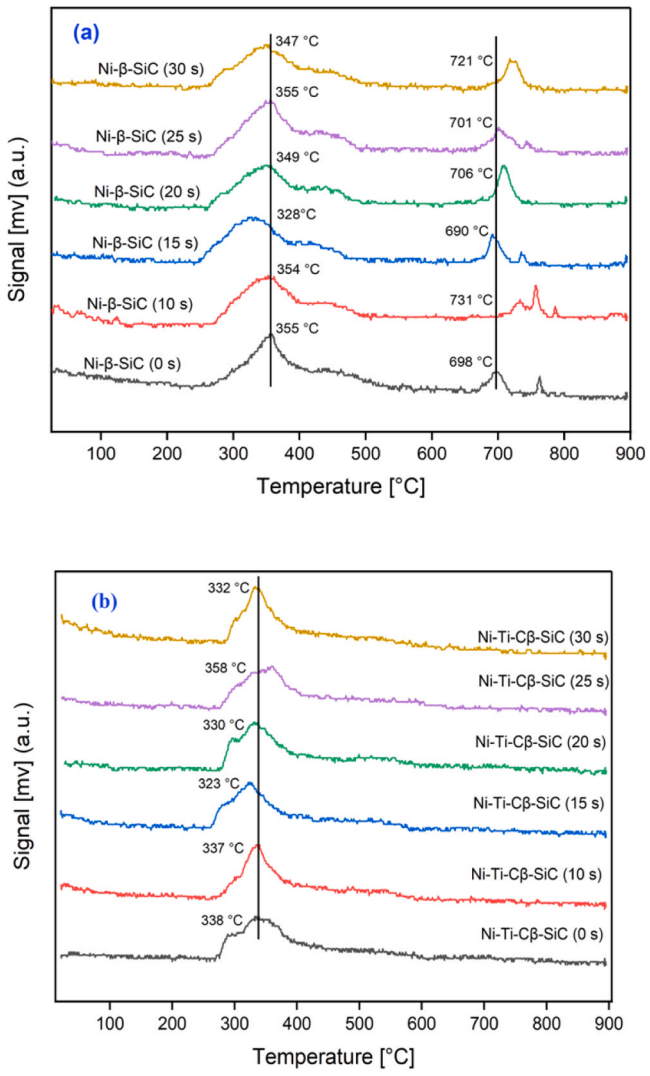

Fig. 6. H_2-TPR of: (a) Ni-β-SiC catalysts; (b) Ni-Ti-Cβ-SiC catalysts.

surface area (79.66 m^2/g vs. 29.02 m^2/g for β-SiC), which promotes better dispersion of the Ni active phase, as confirmed by elemental mapping (Supporting information S1). In addition, the incorporation of Ti and C into the β-SiC support enhances the metal-support interaction, further improving catalytic performance. This observation is consistent with previous reports, such as Liu *et al.* [14], who demonstrated improved activity in Co-based catalysts for Fischer-Tropsch synthesis upon TiO_2 modification of β-SiC.

Despite these advantages, the Ni-Ti-Cβ-SiC catalyst exhibited faster deactivation, likely due to increased carbon deposition at higher conversions. Carbon quantification (Table S1, Fig. 8) revealed that Ni-Ti-Cβ-SiC accumulated more carbon (0.8179 g) than Ni-β-SiC (0.0825 g) after the DRM reaction, supporting the hypothesis that higher activity can lead to increased coking. The main reactions responsible for carbon formation during DRM are methane decomposition, Eq. (5), CO_2 reduction, Eq. (6), and the Boudouard reaction, Eq. (7):

$$CH_4 \leftrightarrow C + 2H_2 \tag{5}$$

$$CO_2 \leftrightarrow CO + C \tag{6}$$

$$CO + H_2 \leftrightarrow H_2O + C \tag{7}$$

Regarding syngas composition, the H_2/CO ratio for Ni-Ti-Cβ-SiC was approximately 0.84 and remained relatively stable until minor fluctuations appeared after 20 h on stream (Fig. 7(c)). For Ni-β-SiC, the H_2/CO ratio was lower (0.71) and exhibited fluctuations from the start of the reaction, reflecting its different catalytic dynamics.

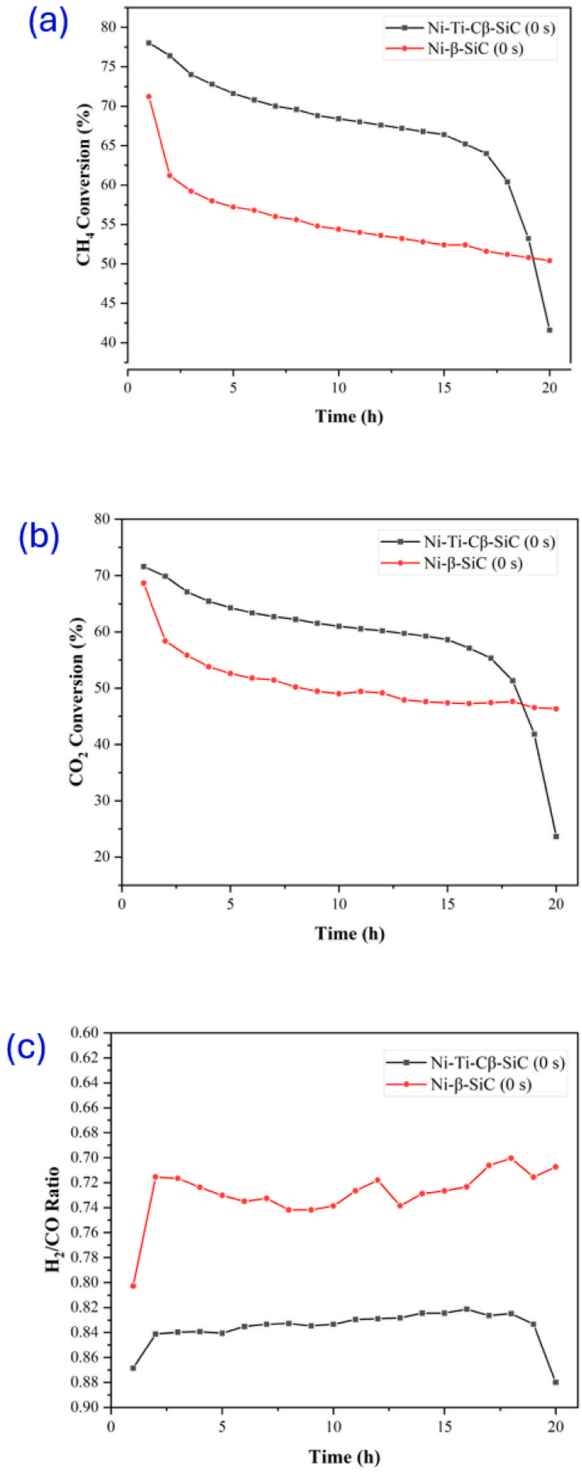

Fig. 7. (a) CH_4 conversions of Ni/SiC catalysts, (b) CO_2 conversions of Ni/SiC catalysts, (c) H_2/CO ratios of Ni/SiC catalysts.

These results highlight the importance of optimizing both the support properties and metal-support interactions to balance activity, stability, and resistance to carbon deposition in DRM catalysts. The findings also underscore the potential trade-off between higher conversion and catalyst longevity, particularly when using supports that enhance Ni dispersion and activity.

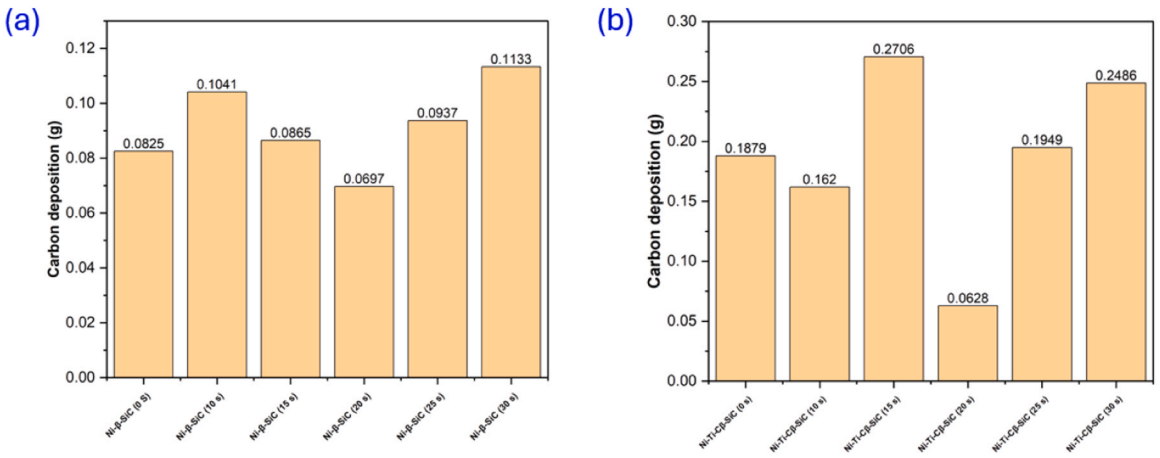

Fig. 8. Carbon deposition test of Ni silicon carbide catalysts after 20 h.

3.2.2. Impact of MIR post-treatment

MIR exposure weakened the Ni-Ti-Cβ-SiC interaction, as evidenced by reduced reduction temperatures in H_2-TPR (Fig. 6(b)). This led to lower CH_4/CO_2 conversions across all treated samples compared to the untreated catalyst (Fig. 9(a), (b)). The Ni-Ti-Cβ-SiC (30 s) catalyst showed the poorest performance, with increased carbon deposition (Table S1, Fig. 8(b)), while the Ni-Ti-Cβ-SiC (15 s) catalyst accumulated the most carbon (0.1879 g), exacerbating deactivation.

H_2/CO ratios for MIR-treated Ni-Ti-Cβ-SiC catalysts (0.72 – 0.78) were lower than the untreated sample (0.84), with progressive declines over time (Fig. 9(c)), most probably because of the lower CH_4 and CO_2 conversions of the MIR-treated Ni-Ti-Cβ-SiC catalysts as compared to the untreated one.

For the β-SiC support, MIR-treated catalysts achieved the highest CH_4 and CO_2 conversions (Fig. 10 (a) and (b)), while all MIR-treated samples showed more stable H_2/CO ratios (Fig. 10 (c)). The Ni-β-SiC (30 s) catalyst, however, proved detrimental, with the lowest CH_4 conversion of 45 % and CO_2 conversion of 42 % with significant carbon deposition (Table S1, Fig. 8(a)), underscoring the need for optimized MIR duration.

In contrast, MIR strengthened Ni-β-SiC interactions, shifting β-type reduction peaks to higher temperatures (Fig. 4(a)). This enhanced stability and activity: the Ni-β-SiC (10 s) and Ni-β-SiC (25 s) catalysts.

4. Conclusion

This study systematically investigated the post-synthesis modification of Ni-β-SiC and Ni-Ti-Cβ-SiC catalysts via MIR for dry reforming of methane. The key findings reveal distinct behaviours between the two catalyst systems, driven by the support composition and MIR-induced structural changes.

Ni-Ti-Cβ-SiC catalyst demonstrated superior initial CH_4 conversion of 65 % and CO_2 conversion 60 % compared to Ni-β-SiC catalyst of CH_4 conversion of 55 % and CO_2 50 %, attributed to their higher surface area and enhanced Ni dispersion facilitated by Ti incorporation. However, rapid deactivation occurred after 15 h on stream due to carbon deposition linked to methane decomposition and CO_2 reduction pathways. MIR exposure weakened Ni-Ti interactions, as evidenced by reduced reduction temperatures, leading to lower activity, but improved stability. Prolonged MIR exposure (30 s) exacerbated carbon formation, highlighting the trade-off between activity and durability.

Ni-β-SiC catalysts, while initially less active, exhibited greater stability. MIR treatment strengthened Ni-β-SiC interactions, shifting β-type reduction peaks to higher temperatures and boosting conversion at optimal exposure times (10 s and 25 s). This enhancement further underscores the role of MIR in tailoring metal-support interactions, which mitigated sintering and improved syngas stability (H2/CO ratio: 076 vs. 0.71 for untreated). However, excessive MIR (30 s) degraded performance, emphasizing the need for precise exposure control.

The contrasting MIR effects on the two catalysts: enhancing Ni-β-SiC while weakening Ni-Ti-Cβ-SiC, highlight the critical influence of support properties on post-treatment outcomes. These findings align with prior studies on MIR's utility in catalytic tuning, but extend its application to SiC-based systems, offering a novel strategy to bypass traditional support modification methods.

Future research will employ advanced characterization methods, such as transmission electron microscopy (TEM) for high-resolution morphology and Ni particle size analysis, and X-ray photoelectron spectroscopy (XPS) to track chemical states and surface oxidation of Ni after MIR treatment. Additionally, we plan to use in-situ and operando techniques including diffuse reflectance infrared Fourier transform spectroscopy (DRIFTS) and X-ray absorption near edge structure (XANES) to directly observe dynamic changes under reaction conditions induced by MIR. Repeatability of the catalytic test should be carried on, as well as systematic studies on MIR parameters, including wavelength, power, and treatment atmosphere, could enable more precise tailoring of catalyst properties and facilitate the integration of MIR processes into scalable reactor design. Expanding the scope to include a broader range of support materials, active metals, and catalyst architectures may reveal new opportunities for enhancing activity and stability. Mechanistic modelling and machine learning could further accelerate optimization of MIR treatment protocols by predicting catalyst behaviour and identifying key performance descriptors. To enhance industrial applicability and provide a more rigorous test of catalyst durability, future work will focus on long-term DRM operation exceeding 100 h. Moreover, we propose to explore in-situ MIR-based regeneration approaches, especially when integrated with renewable energy sources, to maintain catalyst activity and minimize downtime. These steps will be critical for verifying catalyst longevity and ensuring suitability for continuous, sustainable syngas production at commercial scale.

CRediT authorship contribution statement

Kunal Pawar: Investigation, Data curation. **Christel Olivier Lenge Mbuya:** Writing – review & editing, Writing – original draft, Visualization, Validation, Supervision, Methodology, Investigation, Formal analysis, Data curation, Conceptualization. **Harvey Arellano-Garcia:** Writing – review & editing, Writing – original draft, Supervision, Resources, Project administration, Funding acquisition, Conceptualization. **Bogdan Dorneanu:** Writing – review & editing, Writing – original draft, Supervision, Project administration, Methodology, Conceptualization. **Parisa Shafiee:** Writing – review & editing, Visualization, Formal analysis. **Okoye-Chine Chike George:** Writing – review & editing,

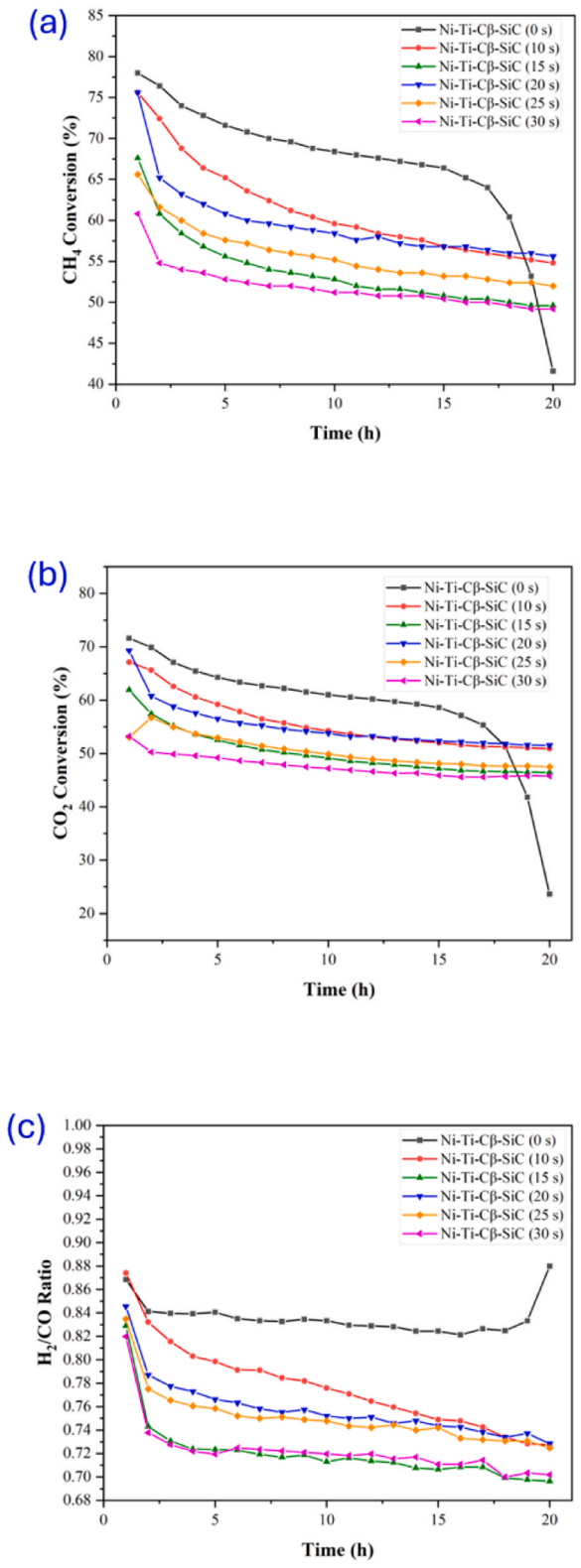

Fig. 9. (a) CH_4 conversions of Ni-Ti-Cβ-SiC catalysts untreated and microwaved, (b) CO_2 conversions of Ni-Ti-Cβ-SiC catalysts untreated and microwaved (c) H_2/CO ratios of Ni-Ti-Cβ-SiC catalysts.

Methodology. **Pilar Tarifa:** Writing – review & editing, Supervision, Methodology, Conceptualization. **Mitra Jafari:** Writing – review & editing, Writing – original draft, Investigation, Formal analysis, Data curation.

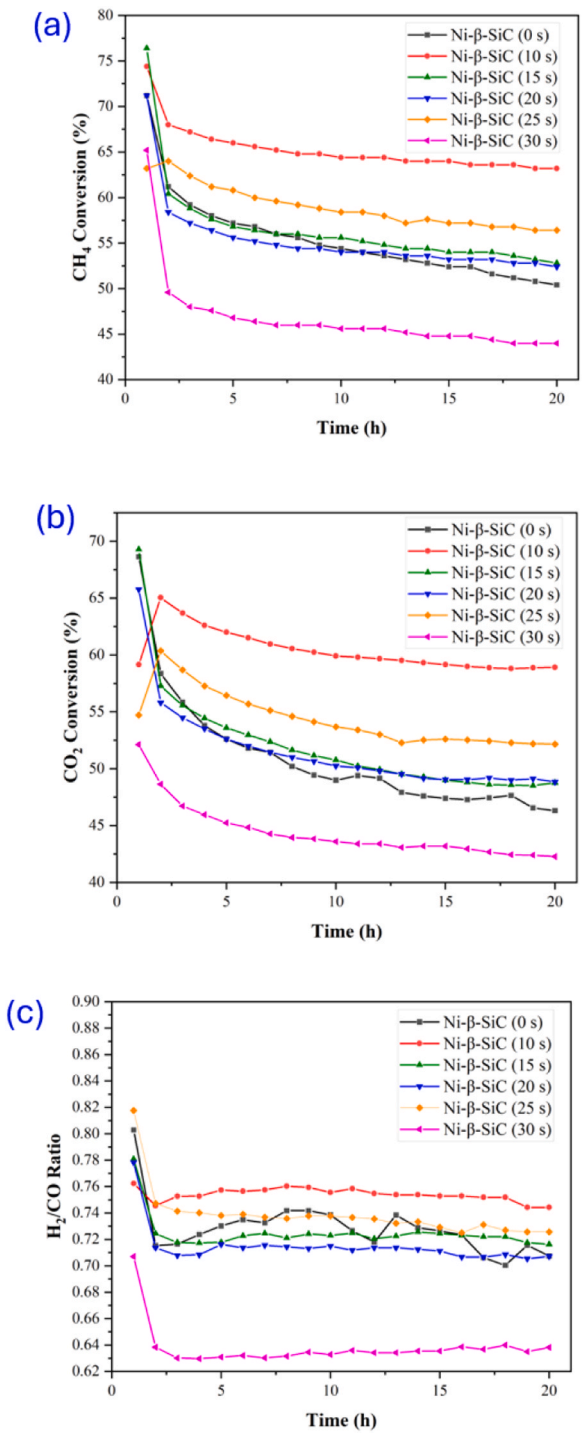

Fig. 10. (a) CH_4 conversions of Ni-β-SiC catalysts untreated and microwaved, (b) CO_2 conversions of Ni-β-SiC catalysts untreated and microwaved (c) H_2/CO ratios of Ni-β-SiC catalysts.

Declaration of Competing Interest

The authors declare that they have no known competing financial interests or personal relationships that could have appeared to influence the work reported in this paper.

Acknowledgements

The financial support of the Bundesministerium für Bildung und Forschung (BMBF) under the project "PyroBioFuel: Sustainable

conversion of biomass into bioenergy through pyrolysis", Grant number 03SF0678, is gratefully acknowledged.

Appendix A. Supporting information

Supplementary data associated with this article can be found in the online version at doi:10.1016/j.jcou.2025.103270.

Data Availability

Data will be made available on request.

References

[1] M.K. Jameel, M.A. Mustafa, H.S. Ahmed, A. jassim Mohammed, H. Ghazy, M. N. Shakir, A.M. Lawas, S. khudhur Mohammed, A.H. Idan, Z.H. Mahmoud, H. Sayadi, E. Kianfar, Biogas: production, properties, applications, economic and challenges: a review, Results Chem. 7 (2024) 101549, https://doi.org/10.1016/j.rechem.2024.101549.

[2] J. Wang, G. Zhang, G. Li, J. Liu, Y. Wang, Y. Xu, Y. Lyu, Understanding structure-activity relationships of the highly active and stable La promoted Co/WC-AC catalyst for methane dry reforming, Int. J. Hydrog. Energy 47 (2022) 7823–7835, https://doi.org/10.1016/j.ijhydene.2021.12.152.

[3] Z. Alipour, V. Babu Borugadda, H. Wang, A.K. Dalai, Syngas production through dry reforming: A review on catalysts and their materials, preparation methods and reactor type, Chem. Eng. J. 452 (2023) 139416, https://doi.org/10.1016/j.cej.2022.139416.

[4] M.S. Ferrandon, C. Byron, G. Celik, Y. Zhang, C. Ni, J. Sloppy, R.A. McCormick, K. Booksh, A.V. Teplyakov, M. Delferro, Grafted nickel-promoter catalysts for dry reforming of methane identified through high-throughput experimentation, Appl. Catal. A Gen. 629 (2022) 118379, https://doi.org/10.1016/j.apcata.2021.118379.

[5] S. Intarasiri, T. Ratana, T. Sornchamni, M. Phongaksorn, S. Tungkamani, Effect of pore size diameter of cobalt supported catalyst on gasoline-diesel selectivity, Energy Procedia 138 (2017) 1035–1040, https://doi.org/10.1016/j.egypro.2017.10.090.

[6] J. Xiao, D. Mao, X. Guo, J. Yu, Effect of TiO 2, ZrO 2, and TiO 2 -ZrO 2 on the performance of CuO-ZnO catalyst for CO 2 hydrogenation to methanol, Appl. Surf. Sci. 338 (2015) 146–153, https://doi.org/10.1016/j.apsusc.2015.02.122.

[7] N. Mota, E.M. Ordoñez, B. Pawelec, J.L.G. Fierro, R.M. Navarro, Direct synthesis of dimethyl ether from co2: Recent advances in bifunctional/hybrid catalytic systems, Catalysts 11 (2021), https://doi.org/10.3390/catal11040411.

[8] C. Jiang, A. Araia, S. Balyan, B. Robinson, S. Brown, A. Caiola, J. Hu, J. Dou, L. M. Neal, F. Li, Kinetic study of Ni-M/CNT catalyst in methane decomposition under microwave irradiation, Appl. Catal. B Environ. 340 (2024) 123255, https://doi.org/10.1016/j.apcatb.2023.123255.

[9] K. Balakrishnan, R.D. Gonzalez, Preparation of Pt/Alumina catalysts by the sol-gel method, J. Catal. 144 (1993) 395–413, https://doi.org/10.1006/jcat.1993.1341.

[10] X. Li, L. Yan, A. Guo, H. Du, F. Hou, J. Liu, Lightweight porous silica-alumina ceramics with ultra-low thermal conductivity, Ceram. Int. 49 (2023) 6479–6486, https://doi.org/10.1016/j.ceramint.2022.10.165.

[11] J.M. Lavoie, Review on dry reforming of methane, a potentially more environmentally-friendly approach to the increasing natural gas exploitation, Front. Chem. 2 (2014) 1–17, https://doi.org/10.3389/fchem.2014.00081.

[12] C.G. Silva, F.B. Passos, V.T. da Silva, Influence of the support on the activity of a supported nickel-promoted molybdenum carbide catalyst for dry reforming of methane, J. Catal. 375 (2019) 507–518, https://doi.org/10.1016/j.jcat.2019.05.024.

[13] J. Sasson Bitters, T. He, E. Nestler, S.D. Senanayake, J.G. Chen, C. Zhang, Utilizing bimetallic catalysts to mitigate coke formation in dry reforming of methane, J. Energy Chem. 68 (2022) 124–142, https://doi.org/10.1016/j.jechem.2021.11.041.

[14] Y. Liu, B. De Tymowski, F. Vigneron, I. Florea, O. Ersen, C. Meny, P. Nguyen, C. Pham, F. Luck, C. Pham-Huu, Titania-decorated silicon carbide-containing cobalt catalyst for fischer-tropsch synthesis, ACS Catal. (2013), https://doi.org/10.1021/cs300729p.

[15] R. Tan, J. Zhou, Z. Yao, B. Wei, Z. Li, A low-cost lightweight microwave absorber: silicon carbide synthesized from tissue, Ceram. Int. 47 (2021) 2077–2085, https://doi.org/10.1016/j.ceramint.2020.09.040.

[16] Z. Zhang, G. Zhao, G. Bi, Y. Guo, J. Xie, Monolithic SiC-foam supported Ni-La2O3 composites for dry reforming of methane with enhanced carbon resistance, Fuel Process. Technol. 212 (2021) 106627, https://doi.org/10.1016/j.fuproc.2020.106627.

[17] L. Bai, H. Xing, W. Chen, P. Yang, X. Ji, Preparation of Ni/C composite microwave absorbers with high performance by controlling nickel source, Colloids Surf. A Physicochem. Eng. Asp. 656 (2023) 130483, https://doi.org/10.1016/j.colsurfa.2022.130483.

[18] C. Ke, T. Liu, Y. Zhang, Q. Xiong, Energy absorption performances of silicon carbide particles during microwave heating process, Chem. Eng. Process. Process. Intensif. 172 (2022) 108796, https://doi.org/10.1016/j.cep.2022.108796.

[19] P. Reubroycharoen, T. Vitidsant, Y. Liu, G. Yang, N. Tsubaki, Highly active Fischer-Tropsch synthesis Co/SiO2 catalysts prepared from microwave irradiation, Catal. Commun. 8 (2007) 375–378, https://doi.org/10.1016/j.catcom.2006.06.031.

[20] S. Abdulridha, Y. Jiao, S. Xu, R. Zhang, Z. Ren, A.A. Garforth, X. Fan, A comparative study on mesoporous Y zeolites prepared by hard-templating and post-synthetic treatment methods, Appl. Catal. A Gen. 612 (2021) 117986, https://doi.org/10.1016/j.apcata.2020.117986.

[21] B. Fidalgo, A. Domínguez, J.J. Pis, J.A. Menéndez, Microwave-assisted dry reforming of methane, Int. J. Hydrog. Energy 33 (2008) 4337–4344, https://doi.org/10.1016/j.ijhydene.2008.05.056.

[22] C.O.L. Mbuya, L.L. Jewell, T.S. Ntelane, M.S. Scurrell, The effect of microwave irradiation on heterogeneous catalysts for Fischer-Tropsch synthesis, Rev. Chem. Eng. 38 (2022) 721–736, https://doi.org/10.1515/revce-2020-0017.

[23] J.A. Díaz, M. Calvo-Serrano, A.R. De La Osa, A.M. García-Minguillán, A. Romero, A. Giroir-Fendler, J.L. Valverde, β-Silicon carbide as a catalyst support in the fischer-tropsch synthesis: Influence of the modification of the support by a pore agent and acidic treatment, Appl. Catal. A Gen. 475 (2014) 82–89, https://doi.org/10.1016/j.apcata.2014.01.021.

[24] J.W. Li, Q. Song, J.B. Li, S.C. Yang, Y.S. Gao, Q. Wang, F. Yu, La-enhanced Ni nanoparticles highly dispersed on SiC for low-temperature CO methanation performance, Rare Met. 40 (2021) 1753–1761, https://doi.org/10.1007/s12598-020-01485-3.

[25] P. Unwiset, K.C. Chanapattharapol, P. Kidkhunthod, Y. Poo-arporn, B. Ohtani, Catalytic activities of titania-supported nickel for carbon-dioxide methanation, Chem. Eng. Sci. 228 (2020) 115955, https://doi.org/10.1016/j.ces.2020.115955.